Journal of Atmospheric and Solar-Terrestrial Physics 105-106 (2013) 170–180

Contents lists available at ScienceDirect

Journal of Atmospheric and Solar-Terrestrial Physics

journal homepage: www.elsevier.com/locate/jastp

Signatures of moderate (M-class) and low (C and B class) intensity solar flares on the equatorial electrojet current: Case studies

D. Chakrabarty [a,*], Mala S. Bagiya [a], Smitha V. Thampi [a], B.M. Pathan [b], R. Sekar [a]

[a] Physical Research Laboratory, Ahmedabad 380009, India
[b] Indian Institute of Geomagnetism, Navi Mumbai 410218, India

ARTICLE INFO

Article history:
Received 16 May 2012
Received in revised form
30 August 2013
Accepted 10 October 2013
Available online 18 October 2013

Keywords:
Solar flare
X-ray flux
EUV flux
Equatorial electrojet
Equatorial ionosphere
Space weather

ABSTRACT

The present investigation brings out, in contrast to the earlier works, the changes in the equatorial electrojet (EEJ) current in response to a few moderate (M-class) and low (C and B class) intensity solar flares during 2005–2010. Special care is taken to pick these flare events in the absence of prompt electric field perturbations associated with geomagnetic storms and substorms that also affect the electrojet current. Interestingly, only the normalized (with respect to the pre-flare level) deviations of daytime EEJ (and not the deviations alone) change linearly with the increases in the EUV and X-ray fluxes. These linear relationships break down during local morning hours when the E-region electric field approaches zero before reversal of polarity. This elicits that the response of EEJ strength corresponding to less-intense flares can be appropriately gauged only when the local time variation of the quiet time E-region zonal electric field is taken into account. The flare events enhanced the EEJ strength irrespective of normal or counter electrojet (CEJ) conditions that shows that solar flares change the E-region ionization density and not the electric field. In addition, the enhancements in the X-ray and EUV fluxes, for these flares occurring during this solar minimum period, are found to be significantly correlated as opposed to the solar maximum period, indicating the differences in the solar processes in different solar epochs.

1. Introduction

The EUV and the X-rays in the solar electromagnetic spectrum contribute to the production of ionospheric plasma. While solar hard X-rays (≤ 0.1 nm) during flare events, H-Lyα (121.6 nm) absorption by NO and cosmic rays, cause the D region ionization, solar soft X-rays in the wavelength range of 0.8–20 nm and UV radiation (79.6–102.7 nm) contribute to the ionization of the E-region. The ionization in the F-region is primarily affected by the radiation in the spectral range of 14.0–79.6 nm. A detailed description on the different regions of solar spectra and their roles in the production of the ionospheric layers is available in Rishbeth and Garriot (1969). The sudden enhancements in EUV and X-ray fluxes during solar flares can cause prompt enhancements in the ionization at the ionospheric heights. The effect of the GOES (Geostationary Operational Environment Satellite) X-class flares (peak flux larger than 10^{-4} W/m^2) on the Earth's ionosphere is quite significant and as a consequence these intense flares have received maximum attention. The enhancement in the ionization at the ionospheric heights in varying degrees due to such intense flares is termed as "crochets" or Solar Flare Effects (SFE) or Sudden Ionospheric Disturbances (SID). SFEs are known to have important ramifications for radio propagations as they can lead to sudden onset of short wave fade out, phase anomaly, shift in the radio frequency, cosmic noise absorption, changes in atmospherics, etc. (e.g. Thome and Wagner, 1971; Mitra, 1974; Donnelly, 1976; Davies, 1990). Most of these effects like short wave fade outs stem from the additional ionization produced primarily in the ionospheric D region by the X-rays associated with flare. In addition, it is also shown that strong flares significantly modulate the currents flowing in the ionospheric E-region (e.g. Raja Rao and Panduranga Rao, 1963; Nagata, 1966; Oshio et al., 1967; Richmond and Venkateswaran, 1971; Rastogi et al., 1999). It is also shown that flares can have significant impact on the F-region electron content (e.g. Mendillo et al., 1974; Tsurutani et al., 2005; Liu et al., 2006; Mahajan et al., 2010), thermospheric densities (e.g. Sutton et al., 2006; Le et al., 2012) and OI 630.0 nm dayglow intensity (Das et al., 2010). Therefore, it has now become apparent that strong X-class flares do have significant impact on all the ionospheric regions.

The underlying reason behind the conspicuous impact of the GOES X-class flares on the low latitude ionosphere is the enormity of the thermal part of the total energy (hot thermal plasma emits soft X-rays) released during these flares. Although non-thermal energies can be as large as thermal energies during a flare (e.g. Saint-Hilaire and Benz, 2005, and references cited therein), it is well-accepted that as one goes from the high (X-class) to moderate (M-class) and low (C or B class) intensity solar flares based on

* Corresponding author. Tel.: +91 79 26314651; fax: +91 79 26314659.
E-mail addresses: dipu.prl@gmail.com, dipu@prl.res.in (D. Chakrabarty).

1364-6826/$ - see front matter © 2013 Elsevier Ltd. All rights reserved.
http://dx.doi.org/10.1016/j.jastp.2013.10.005

GOES soft X-ray measurements, the total thermal energy released will be less in comparison with the high intensity X-class flares. Further, the signatures corresponding to the moderate and low intensity solar flares can get obfuscated by the possible comparable effects due to transient electric field disturbances. Such transient electric field disturbances can occur during storm sudden commencement (e.g. Sastri, 2002), prompt penetration/overshielding events (e.g. Chakrabarty et al., 2006) associated with the polarity reversal of interplanetary electric field (IEF) or substorm (e.g. Chakrabarty et al., 2010). Therefore, in order to unambiguously isolate the signatures of moderate and low intensity solar flares on the ionospheric E-region over low latitudes, it is important to choose flare events when the transient electric field disturbances are absent. It must also be mentioned here that regular ionosonde observations are often inadequate to investigate the effects of solar flare on the ionospheric E-region owing to the lack of sufficient temporal resolution as the change in solar flux associated with solar flare is ephemeral in nature. The presence of the type-II plasma irregularities over the low latitude region and more importantly, the short-wave fade-outs make the ionosonde technique poorly effective in capturing the changes in the density of the ionospheric E-region during flares.

In order to gauge the flare-related changes in the equatorial electrojet current flowing in the dip-equatorial E-region, it is necessary to understand the factors that determine the amplitude of the changes in the EEJ strength. It is known that the ionospheric E-region is characterized by the generation of the solar quiet (S_q) time electric fields (E_{sq}) due to the global scale dynamo action. These electric fields are mapped to the F-region of the ionosphere through the geomagnetic field lines. In the E-region, the motion of the electrons is governed by the strength of the geomagnetic field and thus electrons respond to the $E_{sq} \times B$ drift while the ions move with the neutrals under the influence of collisions resulting in a vertical polarization field. This polarization field forces the electrons to move usually in the westward direction during daytime causing the intense eastward jet of current known as the equatorial electrojet (EEJ). Due to the mutually perpendicular geometry of E_{sq} and B, this effect is most pronounced in a narrow latitudinal belt ($\pm 3^{\circ}$) and at a narrow height region (10 km) centered around 105 km where the Cowling conductivity maximizes. On many occasions, for reasons still being debated, the direction of the EEJ current reverses giving rise to the counter-electrojet (CEJ). As the EEJ strength depends on the available ionization (n) and the plasma drift velocity ($\mathbf{v}$), significant and prompt changes in EEJ are caused by the additional ionization generated during the transient events like solar flares and/or by the perturbation electric field (that can change plasma drift velocity) associated with the space weather events. It is shown that these transient electric field disturbances can alter EEJ significantly (e.g. Kikuchi et al., 2003; Chakrabarty et al., 2010; Simi et al., 2012).

The strength of EEJ is conventionally derived based on ground-based magnetic measurements. Further, the changes in EEJ corresponding to the transient events like moderate and low intensity solar flares can only be captured by magnetic measurements with high precision and cadence. The ground-based measurements of the magnetic field respond to both the solar flare and transient electric field perturbations. Therefore, unambiguous identification of the effects of moderate and low intensity solar flares on the EEJ strength requires careful delineation of the contribution due to the flares from that due to the electric field disturbances. Manju and Viswanathan (2005) investigated a number of flare events and its impact on the E-region current and electric field in the 95–110 km altitude region using VHF (54.95 MHz) coherent backscatter radar observations during daytime from Thumba, a dip equatorial station in India. Although they identified significant changes in the ionospheric E-region over low latitudes corresponding to the X-class solar flares, similar effects could not be identified during M and C class flares. It is to be noted that the magnetometer measurements used by them had lesser cadence and precision. As the strength of the flares is determined based on the X-ray flux and the ionization in the ionospheric E-region depends considerably on the EUV flux, it is important to also understand the relationship between the X-ray and EUV fluxes during these moderate and low intensity solar flares.

There are a number of studies (e.g. Donnelly, 1976; Tsurutani et al., 2005; Leonovich et al., 2010; Mahajan et al., 2010; Le et al., 2011; Zhang et al., 2011) that highlight the discrepancy in the relationship between the solar X-ray and EUV fluxes during flare events. The underlying factor for this discrepancy is pointed out to be associated with the center-to-limb distance (CMD) of the flare location. As the solar EUV radiation originates in the lower solar atmosphere, the absorption of EUV radiation increases as the flare site is located increasingly away from the central meridian. This center-to-limb effect is nominal for the X-ray flux as they originate from the coronal region. This leads to the reduced correlation coefficient between solar X-ray and EUV fluxes during flares. Keeping this in mind, the X-ray fluxes are often adjusted for the CMD factor (multiplied by cos(CMD)) that leads to better correlation. Le et al. (2011) have recently pointed out that the CMD effects for the EUV enhancements are smaller for M and C class flares. However, most of the above-mentioned investigations including the investigation by Le et al. (2011) belong to the solar maximum period.

The solar cycle 23 is characterized by an unusually deep minimum (e.g. Nandi et al., 2011; Broomhall et al., 2009; Bisoi et al., in press) and it is important to investigate how the moderate and low intensity flares affect the equatorial ionosphere during this solar minimum period. In addition, many of the flare events investigated in the earlier reports occurred when geomagnetic storms or substorms were in progress. In order to find the tell-tale ionospheric signatures for the moderate and low intensity flares, it is important to identify and isolate the transient and simultaneously occurring electric field disturbances associated with the storm or substorm events. In the present investigation, a three-pronged approach is adopted to investigate the effects of the moderate and low intensity X-class flares on the equatorial E-region. First, the active regions on the solar disk responsible for these flares are identified so that the relationship between the X-ray and EUV fluxes during these flares occurring during the minimum of the solar cycle 23, is better understood. Second, the interplanetary as well as storm–substorm parameters are carefully analyzed to identify the background geomagnetic conditions so that the possible transient electric field effects on the equatorial E-region can be isolated. Third and the most important one, the relationship between the deviations in the EUV flux during these flares and the associated response in the strength of EEJ is addressed.

2. Data

For the present investigation, the active region maps of the Sun provided by the Mees Solar observatory (http://www.solar.ifa.hawaii.edu/) are used. These maps provide the number of the active region, its location on the visible disk and the area of spots in millionths of the visible hemisphere. The X-ray (0.1–0.8 nm) fluxes (in W m^{-2}) are obtained from the X-ray detectors on-board the Geostationary Operational Environment Satellite (GOES, http://spidr.ngdc.noaa.gov/spidr/) with 1 min cadence. Excess of X-ray flux (ΔX-ray) associated with a flare is taken as the difference between the peak X-ray flux and the pre-flare flux (taken here as the background flux) just prior to the onset of the flare. It is important to note here that the uncertainty in ΔX-ray flux can arise if the GOES algorithm inaccurately captures the onset time of the flare and/or the pre-flare flux level is different from the background flux level. As discussed by Bornmann (1990) and Ryan et al. (2012), the onset time of a flare identified by GOES and through manual inspection may differ leading to errors in the pre-flare flux level. Further, the pre-flare flux level itself may differ from the actual background flux leading to uncertainty in the determination of excess flux. Therefore, background flux correction (e.g. Bornmann, 1990; Ryan et al., 2012) is needed especially when low intensity flares (like B-class flares) occur in the presence of high and varying background. Two limiting scenarios are generally adopted for background subtraction. In the first scenario, it is assumed that the background contribution is zero which implies that the total flux during flare is dominated by the flare itself. This assumption is valid for high intensity flare events when the excess flux increases by orders of magnitude with respect to the background level. In the other scenario, the pre-flare flux is taken as the background flux level. This is what is conventionally adopted to gauge the impact of flares on ionosphere. In reality, the background flux may lie somewhere in between these two limits (e.g. Bornmann, 1990; Ryan et al., 2012). However, deriving this limit using comprehensive algorithms (e.g. Ryan et al., 2012) is a non-trivial job and beyond the scope of the present investigation. Therefore, the pre-flare flux is adopted as the background in the present case.

The EUV fluxes (in photons cm^{-2} s^{-1}) are obtained from the Solar EUV Monitor (SEM) on-board the SOHO satellite (Ogawa et al., 1993). The SEM experiment provides the EUV flux in two spectral bands (26–34 nm and 0.1–50 nm). In order to investigate the impact of the enhancements in the solar EUV flux on the equatorial electrojet, the flux data (http://www.usc.edu/dept/space_science/semdatafolder/semdownload.htm) in 0.1–50 nm spectral channel are used. The cadence of the EUV flux is 15 s. Excess of EUV flux (ΔEUV) associated with a flare is taken as the difference between the peak EUV flux and the pre-flare flux just prior to the onset of the flare. Further, the 1 min data of the dawn-to-dusk component of interplanetary electric field (IEF_Y) are taken from the NASA GSFC CDAWeb (http://cdaweb.gsfc.nasa.gov/istp_public/) wherein the (IEF_Y) data are propagation lag-corrected till the nose of the terrestrial bow shock. In order to compare the IEF_Y data with the ionospheric measurements, the additional propagation time lags owing to the magnetosheath transit time and the Alfven transit time are calculated following the methodology discussed in Chakrabarty et al. (2005) and each datum point in IEF_Y time series is corrected for the additional propagation lags. The Sym-H (ring current index with 1-min temporal resolution) and AL (westward auroral electrojet index) values, taken from WDC-C2 (Kyoto), are also used to check the storm and substorm conditions. The flare events are chosen following a range of criteria. Moderate and low intensity flares occurring on geomagnetically quiet days when $A_P \leq 7$ are identified. Further, during the flare days, the ring current index (Sym-H) remained well within −30 nT. It is also ascertained that the flare events did not occur during periods when SSC (can be determined from the Sym-H variation), and polarity reversal of IEF_Y (dawn-to-dusk component of IEF) as well as substorm activities were absent (denoted by westward auroral electrojet index, AL). Based on the above-mentioned criteria, a few unambiguous cases are investigated.

The ground-based magnetometer data from Tirunelveli (TIR: 8.73°N, 77.8°E, dip angle 2.9°), a station close to the dip equator, and Alibag (ABG: 18.61°N, 72.83°E, dip angle 25.9°), a station sufficiently away from the influence of the electrojet (to subtract the direct magnetospheric effects), have been used to decipher the changes in the equatorial electrojet strength following the methodology suggested by Rastogi and Patil (1986). The precision of the magnetic observations is 0.1 nT. In addition, the temporal resolution of the magnetic measurements is 1 min.

3. Results

Following the stringent selection criteria mentioned in the previous section, 13 medium and low intensity X-ray flares are obtained for the present investigation in which EUV flux data are available for 11 flares. These 11 flare events occur on 6 days during the years 2005, 2007 and 2010. The flare events comprise 9M-class, 3 C-class and 1 B-class flares. Table 1 lists the dates of occurrence of the flares, flaring active region number (in parenthesis) and location, flare category, X-ray flare onset in the Indian Standard Time (IST=UT + 5.5 h), enhancement in the X-ray flux (ΔX-ray in W m^{-2}) in 0.1–0.8 nm spectral channel, enhancement in the EUV flux (ΔEUV in photons cm^{-2} s^{-1}) in 26–34 nm spectral channel, enhancement in the EUV flux (ΔEUV in photons cm^{-2} s^{-1}) in 0.1–50 nm spectral channel, and the changes in the EEJ strength (ΔEEJ in nT). It can be seen from Table 1 that the selected flare events encompass morning, noon, afternoon and evening hours. Although the EUV flux data are not available for 12 February, 2010, this day is still included in this investigation for the reason presented in the discussion section.

Fig. 1 represents the solar active region maps for the six days being investigated here. It can be noticed that the central meridian distances (CMD) of the flare locations are widely different among the flares considered here. For instance, the active regions corresponding to the

Table 1
Dates of occurrence of the flares, flaring active region number (in parenthesis) and location, flare category, X-ray flare onset in the Indian Standard Time (IST=UT + 5.5 h), enhancement in the X-ray flux (ΔX-ray in W m^{-2}) in 0.1–0.8 nm spectral channel, enhancement in the EUV flux (ΔEUV in photons cm^{-2} s^{-1}) in 26–34 nm spectral channel, enhancement in the EUV flux (ΔEUV in photons cm^{-2} s^{-1}) in 0.1–50 nm spectral channel, changes in the EEJ strength (ΔEEJ in nT).

Date	(AR) Location	Category	Onset (IST)	$\Delta X_{0.1-0.8\ nm}$	$\Delta EUV_{26-34\ nm}$	$\Delta EUV_{0.1-50\ nm}$	ΔEEJ
28 August 2005	(0803) N09E36	M1.6/SF	15.79	1.59E−05	1.00E+09	6.00E+9	4.65
02 June 2007	(0960) S09E77	M2.5/SF	10.65	2.88E−5	3.00E+08	7.00E+9	23.55
	(0960) S09E77	M1.0/SF	15.98	1.09E−5	2.00E+08	4.00E+9	−5.00
03 June 2007	(0960) S10E68	M7.0/SB	7.35	7.88E−5	2.20E+09	1.59E+10	2.38
	(0960) S06E63	M4.5/SF	12.10	5.24E−5	1.60E+09	9.70E+9	12.65
07 February 2010	(1045) N21E10	M6.4/1N	7.8	6.46E−5	1.30E+09	1.18E+10	2.35
	(1045) N21E07	B7.4/SF	13.45	5.79E−7	2.00E+08	5.00E+8	1.35
08 February 2010	(1045) N25E00	C7.7/SF	9.37	7.07E−6	3.00E+08	2.40E+9	4.75
	(1045) N21W01	C6.8/SF	11.45	5.73E−6	5.00E+08	2.00E+9	4.09
	(1045) N21W03	M4.0/SF	13.08	4.04E−5	8.00E+08	8.80E+9	11.43
	(1045) N21W03	M1.1/SF	17.45	1.10E−5	3.00E+08	2.70E+9	1.42
12 February 2010	(1046) N24E13	C7.9/1N	12.9	7.80E−6	No data	No data	6.04
	(1046) N26E11	M8.3/1N	16.92	8.73E−5	No data	No data	3.96

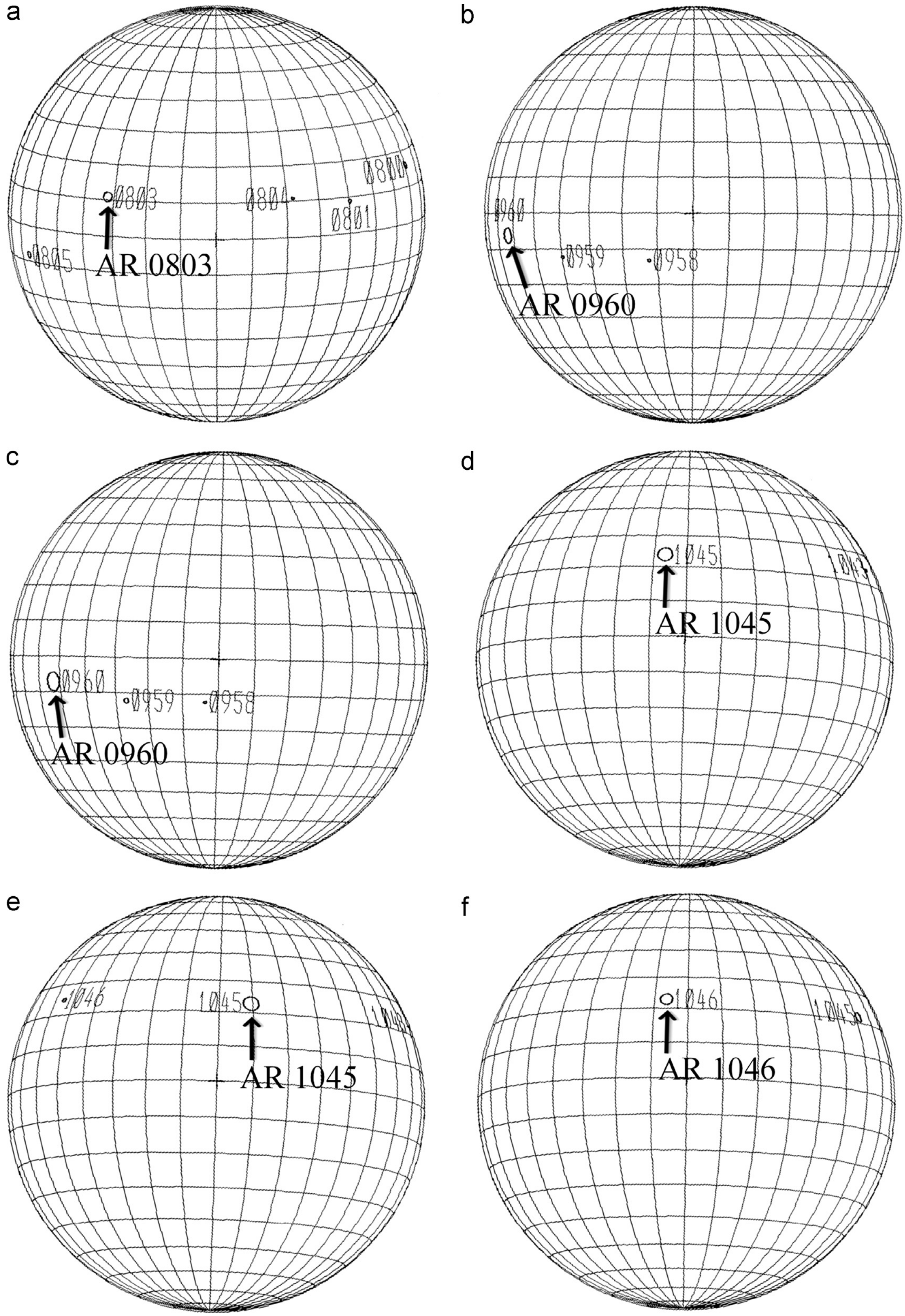

Fig. 1. The flaring active regions on the solar disk are marked by arrows for the six days. Note that the number of active regions on the visible disk (at 16:32:07 UT) is generally 2 or 3 on these days except on 28 August 2005 where the number of active regions is 5.

7, 8 and 12 February 2010 flares were located between the E10 and W03 longitudes whereas the active region was located at E36 longitude for the 28 August 2005 flare (see Table 1). The active region is quite far from the central meridian for the flares during 2–3 June. During this period, the location of the active region varied between E77 and E63 longitudes. Fig. 2a and b shows the linear regression analyses between the ΔX-ray (0.1–0.8 nm) and ΔEUV fluxes obtained from the two spectral channels (26–34 nm and 0.1–50 nm) respectively for the 11 flares when both X-ray and EUV fluxes are available. The correlation coefficients (R) turn out to be 0.89 and 0.98 in the two

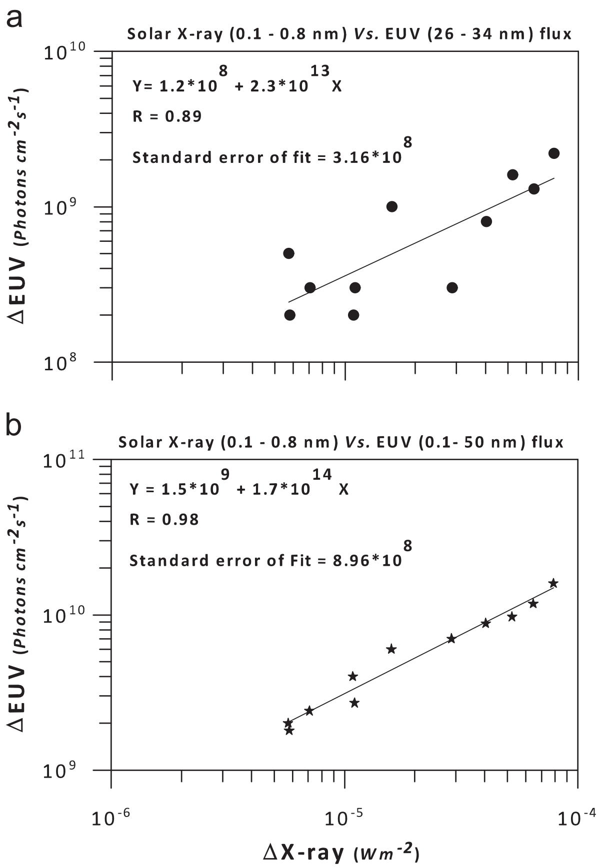

Fig. 2. The linear regression analyses between the ΔX-ray and (a) ΔEUV (26–34 nm) flux and (b) ΔEUV (0.1–50 nm) flux for all the medium and low intensity solar flares when the data of X-ray and EUV fluxes are simultaneously available. Correlation coefficients of 0.89 and 0.98 are obtained for (a) and (b) respectively.

cases as shown in Fig. 2a and b respectively. The implication of this result will be addressed in Section 4.

Fig. 3 shows three panels where the left panel in each row shows the variation of the propagation lag-corrected IEF_Y (in mV/m) whereas the middle and the right panel bring out the variations in AL index and Sym-H respectively during the six days under consideration. In each of these panels, the onset of the EUV flares is marked by arrows. It is important to note that the flare events occur during the periods when sharp polarity reversals in IEF_Y along with intensifications in AL and Sym-H are absent. Storm sudden commencements (SSC) are also not observed during the flare periods. This enables us to realistically assume that the responses of the EEJ corresponding to the enhancements in the solar EUV flux are devoid of any possible influences arising out of the transient electric field disturbances associated with SSC, storm or substorm. It is important to note here that many flare events are scrutinized and disregarded owing to the concomitant presence of storm and/or substorm. This limits the number of unambiguous cases needed to capture the signatures of medium and low intensity flares on the EEJ strength. In order to highlight this aspect, a couple of events are presented in Fig. 4. The figure shows the M3.4 class (Location: S11E33, Active region: 0794) and the M8.9 class (Location S09E36, Active region: 0960) flare events on 03 August 2005 (A_P=7) and 04 June 2007 (A_P=12) on the left and right panels respectively. Associated changes in the X-ray and EUV fluxes, IEF_Y, AL and EEJ strengths for these two days are presented on the left and right panels of this figure. The vertical lines in both the panels reveal the onset of positive deviations in the EEJ strength and the solar fluxes. However, the flare periods are also marked by substorm recovery phases (as indicated by AL) during which electric field disturbances are possible. Therefore, the flare events concomitant with significant depressions in AL and Sym-H are not considered for the present investigation.

Figs. 5 and 6 present the flare events that are considered for the present investigation. The responses of EEJ during the M-class flare events that occurred on 28 August 2005 and 02–03 June 2007 are depicted in Fig. 5. The first and second rows of Fig. 5 bring out the variations in X-ray and EUV fluxes on these days whereas the third row shows the variations in the EEJ strength (in nT). Conspicuous signatures (marked by arrows) are noticed in the EEJ strength corresponding to the flare events labeled in the top row. Interestingly, when the EEJ is negative (westward polarity, CEJ), as is the case at 15.98 h IST on 02 June 2007, the M1.0/SF class flare event makes it further negative. During the other flare events that encompass morning and noon hours, the flares cause positive deviations in the EEJ strength. Importantly, although the amplitude of the change in the EEJ strength corresponding to the M1.6/SF class flare at 15.79 h IST on 28 August 2005 stands out, the corresponding signature for a stronger flare (M7.0/SB class) at 7.35 h IST on 03 June 2007 appears to be relatively disproportionate. In addition, the large positive deviation (by ~24 nT) of EEJ strength corresponding to the M2.5/SF flare at 10.65 IST on 02 June 2007 is also particularly striking despite the fact that the temporal pattern (two-step increase) of the EEJ variation during this flare follows the temporal patterns of X-ray and EUV flux enhancements.

Fig. 6 highlights the flare events during February 2010 and their effects on the EEJ strength. These flares (comprising C and B-class flares also) occur during morning, afternoon and evening hours. Similar to Fig. 5, the first and second rows of Fig. 6 elicit the variations in the X-ray and EUV fluxes whereas the third row brings out the variations in the EEJ strength (in nT). Conspicuous positive deviations are observed in the EEJ strength corresponding to all the marked flares (top row) except during C9.9/1F flare on 07 February 2010 that starts at 10.27 h IST. The onset of this flare is marked by a vertical dashed-line. A significant positive deviation in the EEJ strength is seen that starts at ~10.60 IST, almost 30 min after the occurrence of the C9.9/1F flare. The time delay of this magnitude is not expected as far as the response of the terrestrial E-region corresponding to solar flare is concerned and the possible reason for this variation in the EEJ strength is addressed in the discussion section. Further, it is interesting that the change in the EEJ strength corresponding to the M1.1/SF class flare at 17.45 h IST on 08 February 2010 is conspicuous whereas the corresponding signature for a much stronger flare (M6.4/1N class) at 7.80 IST on 07 February 2010 appears to be relatively disproportionate.

In order to explore the causal connection between the enhancements in the EEJ strength (ΔEEJ) with the enhancements in the X-ray flux (ΔX-ray) and EUV flux (ΔEUV) respectively, correlation analyses of ΔEEJ are performed with ΔX-ray (Fig. 7a) and ΔEUV (Fig. 7c). Very poor correlation coefficients (0.03 and 0.15 respectively) are obtained in both the analyses that indicate that ΔEEJ is not correlated with either ΔX-ray or ΔEUV. However, when correlation analyses are performed between $\Delta EEJ/EEJ_{pre-flare}$ (enhancement in the EEJ strength normalized to the pre-flare EEJ level) with ΔX-ray and ΔEUV, significantly high correlation coefficients of 0.77 and 0.80 are obtained respectively). The implications of these results will be discussed in the ensuing section.

4. Discussion

As mentioned in the Introduction section, the EEJ current flows primarily in a narrow height region (10 km) centered around 105 km in the ionospheric E-region. The peak production of ionization in the E-region (~100–140 km) of the ionosphere also

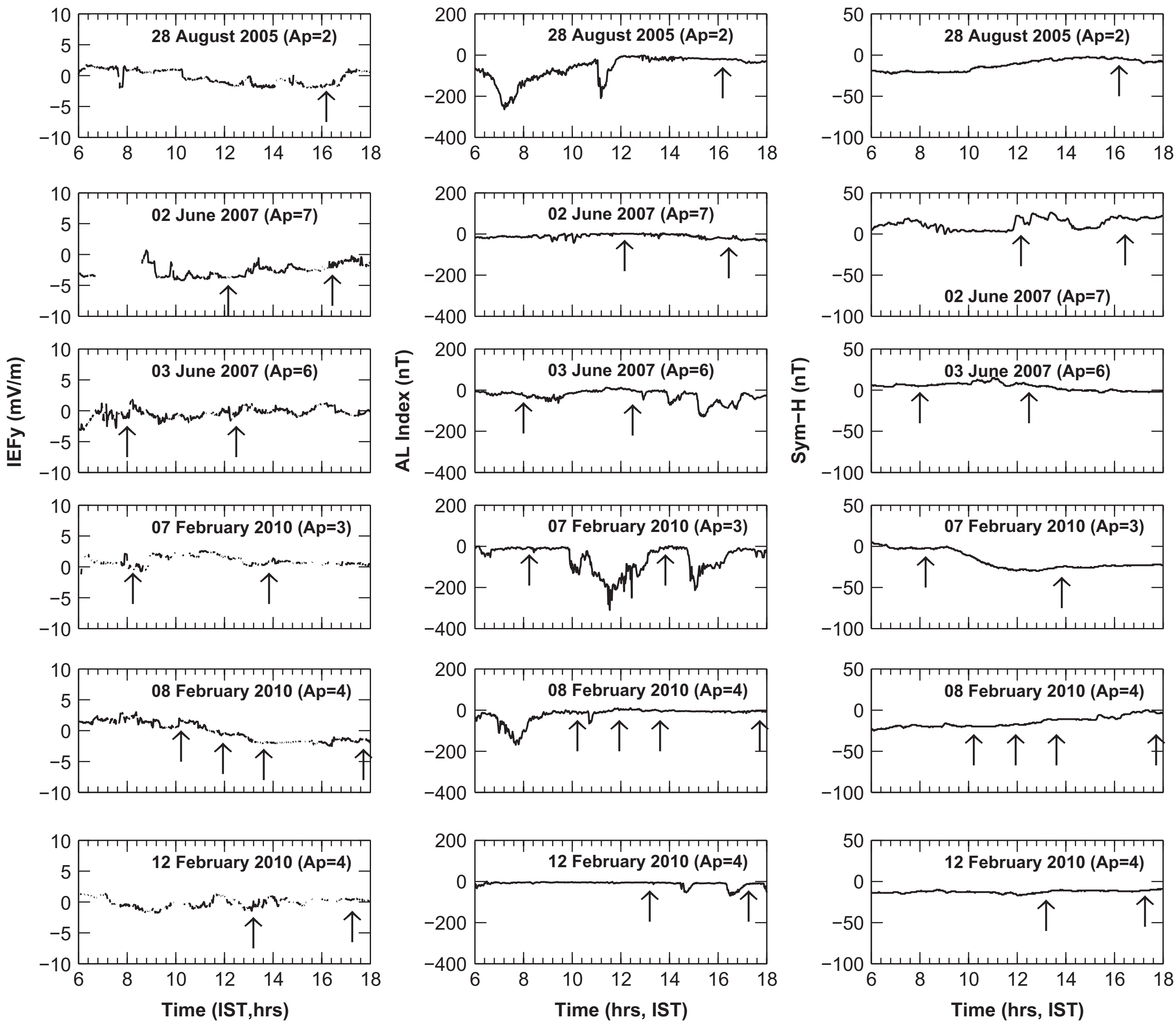

Fig. 3. The variations in IEF_Y (left panel), AL (middle panel) and Sym-H (right panel) for the six days under consideration. The time of occurrence of the flares under consideration is marked by upward arrows. Indian Standard Time, IST=Universal Time, UT + 5.5 h.

occurs around 105–110 km as can be verified from the electron density profiles over the dip equator. The production of ionization at the altitude region of 100–110 km is governed primarily by the photoionization of O_2 by the solar H Lyman-β line (102.6 nm) and photo-ionization of all atmospheric gases (mostly N_2) by solar soft X-rays in the ~1–20 nm range (Solomon, 2006). Using model calculations, it is, in fact, argued by Solomon (2006) that the soft X-rays play a very important role in the ionization process at the E-region altitudes. Therefore, for the present investigation, the flux data from the 0.1-50 nm EUV channel is more relevant.

Importantly, the solar flux measured by the 0.1–50 nm EUV spectral channel captures the soft X-ray (0.1–0.8 nm) emissions in addition to the EUV emissions. Therefore, significant correlation (R=0.98) between the EUV (0.1–50 nm) and the X-ray (0.1–0.8 nm) flux may indicate toward the X-ray contribution in 0.1–50 nm spectral channel (Fig. 2b). However, Fig. 2a suggests that the significant correlation between EUV and X-ray fluxes is not solely a contamination issue. Fig. 2a shows that substantial correlation (R=0.89) exists between the two independent channels, i.e. the 26–34 nm EUV and 0.1–0.8 nm X-ray channels. This suggests that the correlation between X-ray and EUV fluxes in the present case is associated with solar processes especially because the solar X-ray and EUV emissions are known to emanate from different parts of the solar atmosphere. While the X-ray emission primarily comes from the coronal region, the EUV emission originates mainly from the lower solar atmosphere.

The good correlation between the solar EUV and X-ray fluxes is a significant result particularly because many of the recent results (e.g. Afraimovich et al., 2002; Tsurutani et al., 2005; Liu et al., 2006; Leonovich et al., 2010; Mahajan et al., 2010; Le et al., 2011) bring out the spectral difference between the ΔX-ray and ΔEUV fluxes during solar flares suggesting that the X-ray flux is not always a good “proxy” for the solar EUV flux. It is also shown (e.g. Mahajan et al., 2010) that the X-ray fluxes, adjusted for the CMD factor (multiplied by cos(CMD)), leads to better correlation with the EUV fluxes. Interestingly, most of the above-mentioned studies are carried out during solar maximum conditions when the solar active regions are large in number and the contribution of the EUV

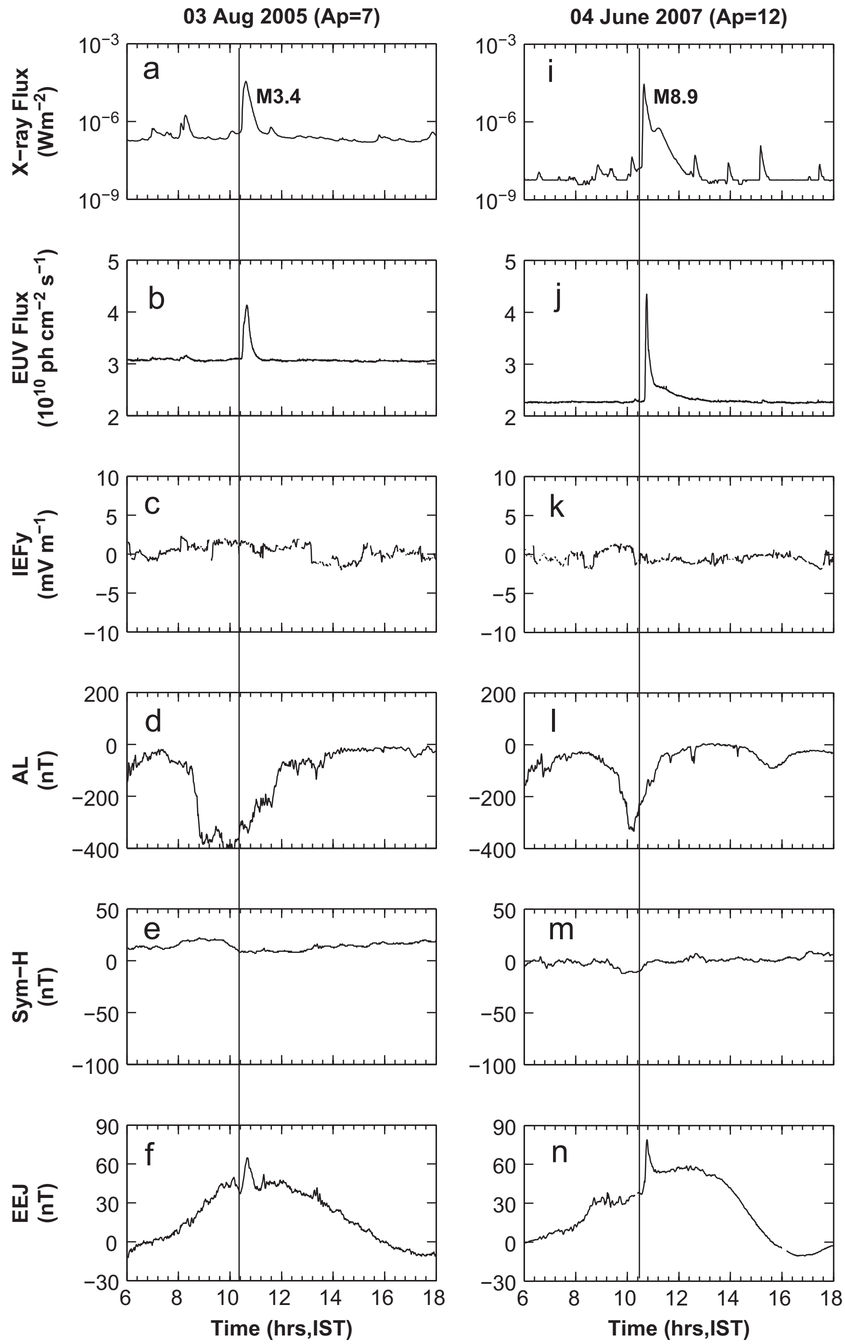

Fig. 4. Many moderate and low intensity flares are not selected for the present investigation to avoid ambiguity. The flares like M3.4 flare on 03 August 2005 (left panel) and M8.9 flare on 04 June 2007 (right panel) are presented as typical examples when concomitant electric field disturbances over dip equator due to magnetospheric substorms (inferred based on AL index) cannot be ruled out despite the absence of geomagnetic storms (inferred based on Sym-H index).

flux from the non-flaring active regions on the solar disk cannot be neglected. There are some earlier works (e.g. Horan and Kreplin, 1981; Horan et al., 1983) that suggested good correlation between ΔX-ray and ΔEUV fluxes during low solar activity periods. In the present investigation, the relatively high correlation coefficients (0.89 and 0.98) obtained between ΔX-ray and ΔEUV fluxes can arise for two reasons. Firstly, for lesser rank X-ray flares (M, C and B-classes), the CMD effect can be inherently less as suggested by Le et al. (2011). Secondly, the flares under consideration here occurred during the minimum activity period of solar cycle 23 under geomagnetically quiescent conditions when the active regions especially in the solar limb are relatively less (Fig. 1). Therefore, the CMD effect for the absorption of the EUV emission is less leading to relatively high correlation between ΔX-ray and ΔEUV fluxes.

In addition to the flare-related changes in the EEJ strength, the effects of the penetration electric fields during geomagnetic storm, SSC and substorm occurring around the time of the flares may also change the strength of EEJ. For X-class flares, this may not pose a serious problem as the magnitude of the flare-induced changes is significantly large and conspicuous. However, for medium and low intensity flares (like M, C, B class of flares), this is a necessity as the magnitude of the changes in the EEJ strength during these flares can be comparable with those caused possibly by the penetration electric fields. This is amply demonstrated by the significant positive deviation in the EEJ strength that starts at 10.27 h IST on

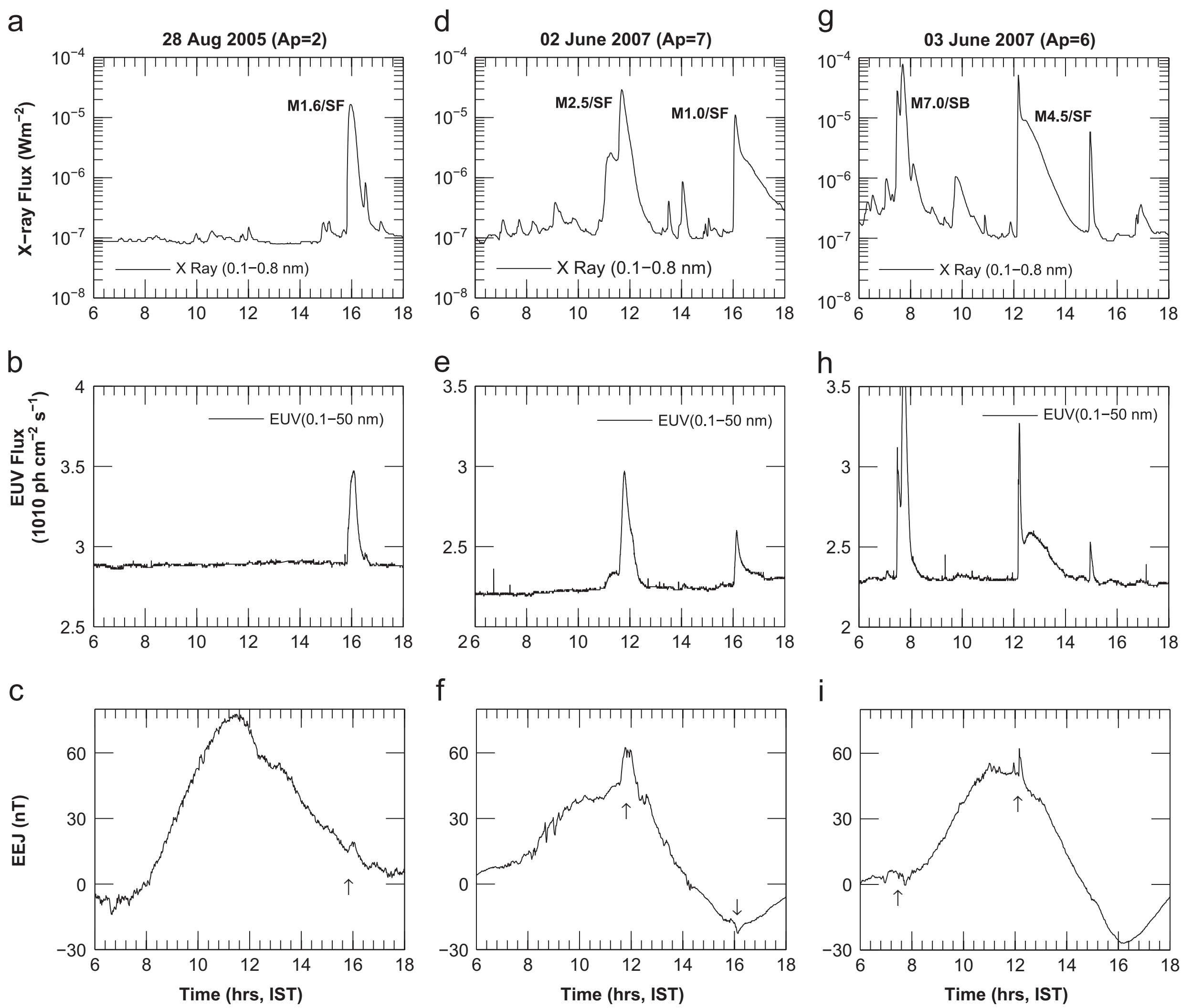

Fig. 5. The variations in the X-ray flux (top row), EUV flux (middle row) and EEJ strength (bottom row) for the representative flares in 2005 and 2007. The flares under consideration are marked at the top row and the corresponding variations in the EEJ strength are marked by arrows in the bottom row. Indian Standard Time, IST=Universal Time, UT + 5.5 h.

07 February 2010. This deviation in the EEJ strength occurs almost 30 min after the occurrence of the C9.9/1F flare on this day. As the relaxation time of the ionospheric response during a solar flare event is of the order of 1 min (Baker and Davies, 1966), this deviation in EEJ cannot be attributed to the C9.9/1F class flare. Interestingly, by closely scrutinizing the AL variation (Fig. 3) at this time on 07 February 2010, one can observe the development of the expansion phase of a substorm event. Daytime electric field enhancement in the strength of the EEJ over Indian region due to the onset of the expansion phase of a magnetospheric substorm has been shown by Chakrabarty et al. (2010). Therefore, this enhancement in EEJ strength could very well be due to the substorm-related electric field disturbance. Therefore, it is imperative that one needs to be more careful to address the effects of lesser rank (M, C and B class) flares on the EEJ. To the best of our knowledge, no other earlier work considered this aspect critically. As the present flare events fall under magnetically quiescent conditions and the effects of penetration electric fields are ruled out, even the small changes in the EEJ strength during the times of the lesser rank flares can be safely identified. Moreover, as the cadence of the magnetic data is 1 min and precision of the measurements is 0.1 nT, these tiny variations are unambiguous. As mentioned in the Introduction section, cadence and precision of this order are difficult to obtain based on the other technique like ionosonde. Therefore, in the absence of electric field disturbances, these tiny variations in the EEJ strength can be attributed to the changes in the E-region electron density by the enhancements in the EUV and soft X-ray radiation. It must be noted in this context that the M8.3/1N flare on 12 February 2010 (Fig. 6i) causes positive deviation when the EEJ strength is barely positive and the M1.0/SF flare event on 02 June 2007 (Fig. 5f) causes negative deviation when EEJ strength is negative (CEJ condition) although these flare events are separated in local time by only about an hour. This is a clear evidence that the flare changes the ionization of the E-region and polarity of the electric field does not get affected. In the absence of EUV flux on 12 February 2010, the enhancement in the X-ray flux can be taken as marker as the EUV flux and the X-ray flux are shown to be in correspondence with each other in the present investigation. This is a reasonable inference as soft X-rays play an important role in the E-region ionization. Although the changes in the E-region ionization density due to strong flare events are shown earlier (e.g. Rastogi et al., 1999; Onwumechili, 1997), the present investigation unambiguously reveals the changes in the E-region ionization density during medium and low intensity flares.

One of the interesting aspects of the present investigation is the lack of correlation of ΔEEJ with both ΔX-ray (Fig. 7a) and ΔEUV (Fig. 7c) fluxes. This is surprising as Figs. 5 and 6 clearly show that the

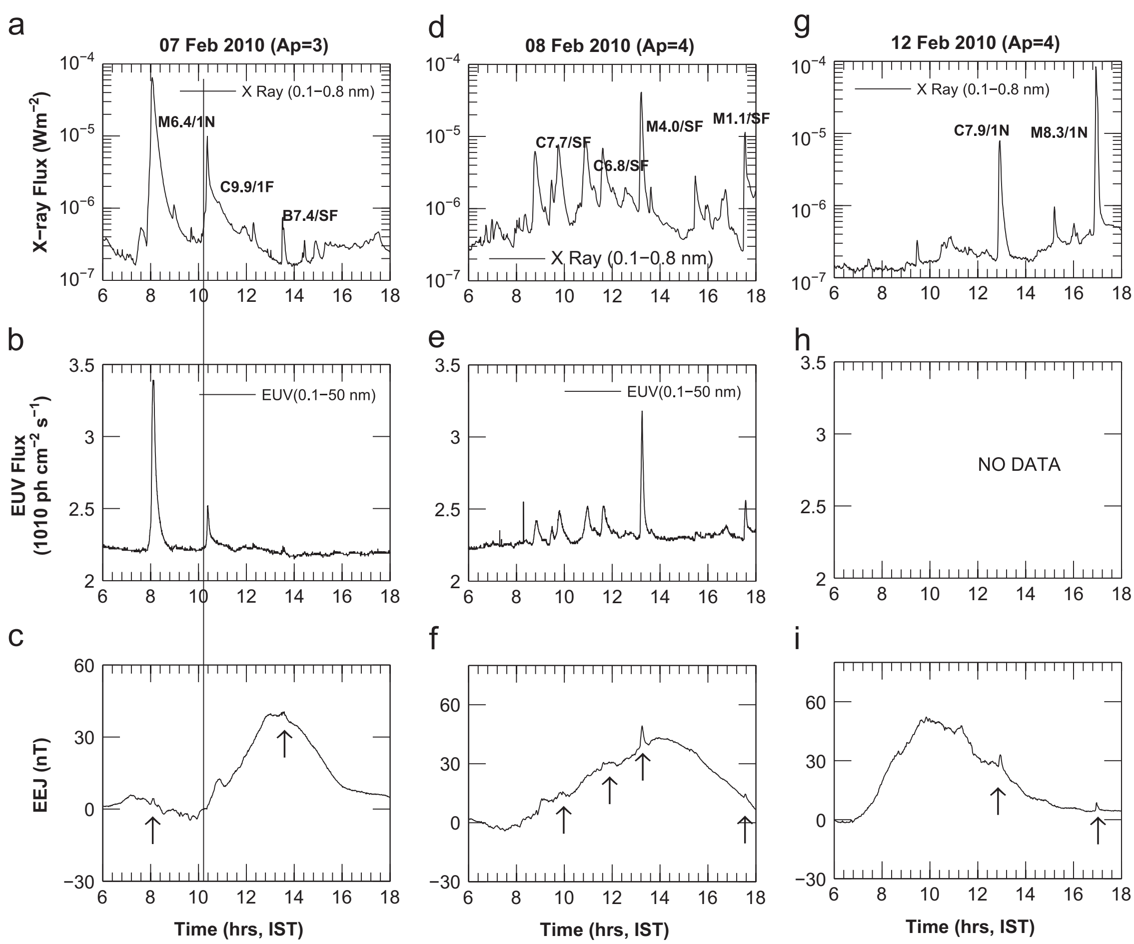

Fig. 6. Same as Fig. 4 but for the year 2010. The vertical dashed line shows the onset time of the C9.9/1F flare on 07 February 2010. Note a peak in the EEJ strength after ~30 min of the occurrence of the peak of the flare. As the relaxation time of the ionospheric response is of the order of 1 min, this EEJ enhancement cannot be attributed to the C-class flare.

strengths of the EEJ current respond almost instantaneously to the enhancements in the X-ray and EUV fluxes during all the marked flares. Interestingly, significant correlation of $\Delta EEJ/EEJ_{pre-flare}$ is found with both ΔX-ray as well as with ΔEUV. If one assumes that the E-region electric field does not change (which is a reasonable assumption) during the period when the X-ray and EUV fluxes reach their maximum values, the enhancement in the EEJ strength normalized to the pre-flare level stands only for the fractional changes in the E-region ionization during the interval of the flare. As the ground magnetic signatures of EEJ are due to the changes in the E-region currents, ΔEEJ depends not only on the available ionization but also on the S_q (solar quiet time) electric field. The S_q electric field over low latitudes has a large local time variation. Based on the combined incoherent scatter radar observations at Jicamarca and Ion Drift Meter observations on-board the Atmospheric Explorer E satellite, Scherliess and Fejer (1999) formulated a global empirical model for the quiet time F-region equatorial vertical drift. This climatological model results show that the average F-region vertical plasma drift reverses polarity and crosses null-point over Indian longitudes in the morning hours under geomagnetically quiescent conditions. It is known that the zonal S_q electric field (E_{sq}) drives the F-region vertical drift as well as the E-region horizontal plasma drift. Therefore, as the zonal S_q electric field (E_{sq}) approaches null-point during the course of the polarity reversal, the E-region plasma drift also approaches a very low value. This, in turn, will make the EEJ current negligible even if strong enhancements in the ionization density are caused by the presence of strong solar flares during that time. This is amply evident if one compares the disproportionately small response of the EEJ strength corresponding to the M6.4/1N flare at 7.8 h IST on 07 February 2010 in comparison with the M1.1/SF flare at 17.45 h IST on 08 February 2010. Disproportionate change in the EEJ strength is also noticed during the M7.0/SB class flare at 07.35 IST on 03 June, 2007. Therefore, it is clear that these disproportionate responses of EEJ strength occur at ~0800 h local time when the E-region zonal electric field is close to zero. Further, production and loss processes are not expected to be significantly different during morning and evening hours so that EEJ response corresponding to these flares can differ significantly during morning and evening hours. In order to further understand this aspect, the IRI-2007 model (Bilitza, 2001) output (not shown here) is used. The model output reveals that the variation in the electron density over Indian dip equatorial region is quite symmetrical with increasing and decreasing electron density during early morning and evening hours respectively on the flare days. As the IRI-2007 model is expected to capture the production process quite efficiently, it is evident that the production process is not responsible for the different responses of the E-region during morning and evening hours. As the location of the active region does not change significantly between 07 and 08 February 2010, it is unlikely that the CMD effect (absorption of EUV flux) has played any role for the disproportionate EEJ responses during the morning and evening hours. Therefore, the magnitude of the E-region zonal electric field is an important factor that has a discernable effect on the response of the EEJ strength particularly during medium and low intensity solar flares.

The definitive role of the E-region electric field in deciding the amplitude of change in the EEJ strength corresponding to medium and low intensity flares is further indicated by the observation of

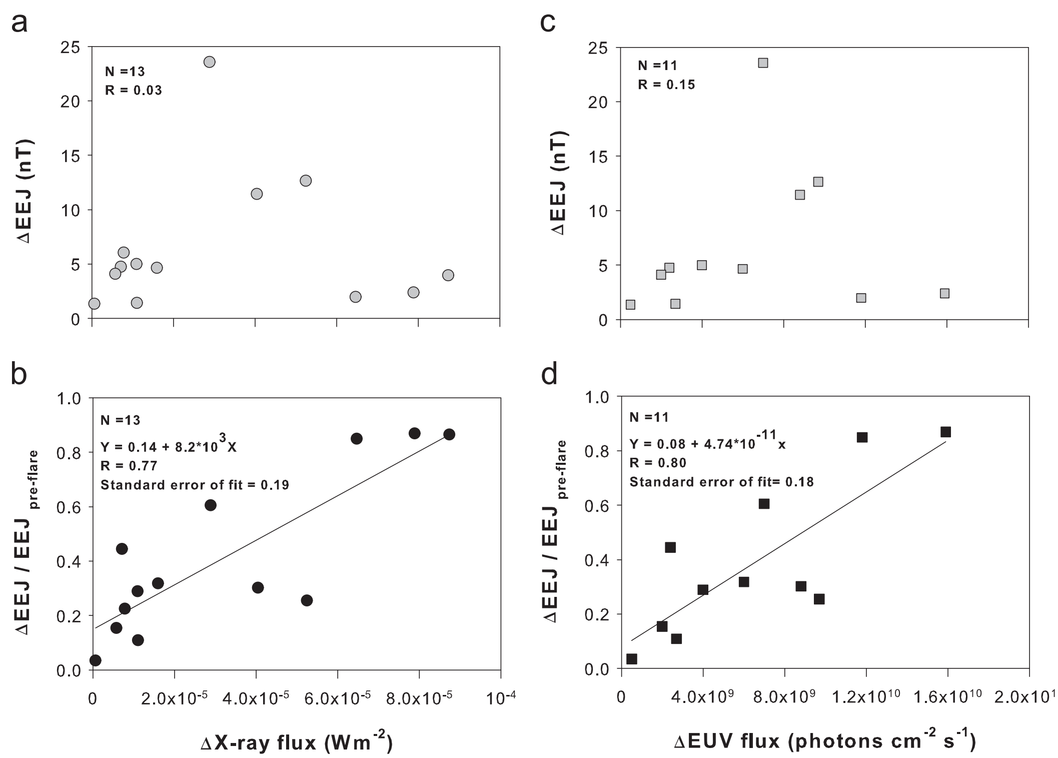

Fig. 7. ΔEEJ, not normalized to the pre-flare level, is not correlated with (a) ΔX-ray and (c) ΔEUV respectively. Correlation improves significantly when ΔEEJ is normalized to the respective pre-flare levels. Correlation coefficients are 0.77 for (b) and 0.80 for (d) respectively.

the large positive deviation (by ~24 nT) of EEJ strength corresponding to the M2.5/SF flare at 10.65 IST on 02 June 2007. The similarities in the temporal patterns (two-step increase) of the EEJ strength with those of the X-ray and EUV fluxes during this flare interval suggest causal connection between the flare event and the changes in the EEJ strength. However, the large magnitude of the change in the EEJ strength is expected to be due to the combined effects of the flare and the large magnitude of the drift velocity of plasma (as a consequence of increasing magnitude of the zonal electric field) at this local time. This suggestion gets support from Fig. 7. In Fig. 7a, ΔEEJ=23.55 stands distinctly apart from the rest of the points whereas it becomes more consistent with the rest of the points once normalized with the pre-flare level.

In the end, it must be re-emphasized that the effects of solar flares on terrestrial ionosphere are, more often than not, accompanied by storm and substorm events. The response of ionosphere corresponding to the transient events like moderate and low intensity solar flares can only be gauged by magnetic measurements with high precision and cadence. However, the magnetic measurements over low latitudes respond to the electron density variation caused by the flare events and also to the changes in the electric fields associated with storms/substorms in addition to the local time variation of the E-region zonal electric field. Thus, the present investigation shows a way to delineate the effects due to the lesser rank flare events on the equatorial electrojet. Earlier investigations did not consider these aspects. As isolated solar flare events without storms/substorms are limited, a few case studies are undertaken in the present investigation that revealed even moderate and low intensity solar flares do affect the equatorial electrojet. It also brings out that the local time variation of ionospheric electric field needs to be properly accounted for in order to investigate the relationship between the amplitude of deviation of the electrojet strength with the strength of the flare. Therefore, this investigation paves way for the detailed studies in future that will address the impact of flare events on the electrojet using simultaneous magnetometer and electric field (using radar) measurements.

5. Summary

It is shown that the significant correlation can exist between the ΔX-ray and ΔEUV fluxes during solar flares when the non-flaring active regions are less in number. Based on the high resolution magnetic measurements over the Indian region, it is demonstrated that the signatures of the medium and low intensity flares on the equatorial electrojet can be identified unambiguously and the deviations in the EEJ strength are due to the enhanced E-region ionizations caused by these flares. It is elicited that the deviations in the EEJ strength corresponding to solar flare events are modulated by the E-region electric field and this becomes particularly significant at the time of the medium (M-class) and low (C and B -class) intensity X-ray flares.

Acknowledgments

The authors thank the Mees Solar observatory, SOHO/SEM and the GOES-10 team for the solar data. The authors would also like to thank the NASA GSFC CDAWeb team for the solar wind data and WDC-C2 (Kyoto) for the auroral electrojet and geomagnetic indices data. This work is done as part of the CAWSES-India programme and is supported by the Department of Space, Government of India.

References

Afraimovich, E.L., Altynsev, A.T., Grechnev, V.C., Leonovich, L.A., 2002. The response of the ionosphere to faint and bright solar flares as deduced from global GPS data. Ann. Geophys. 45, 31–40.
Baker, D.M., Davies, K., 1966. Solar flare effects and the relaxation time of the ionosphere. J. Geophys. Res. 71, 2840–2842.
Bilitza, D., 2001. International reference ionosphere 2000. Radio Sci. 36, 261–275.
Bisoi S.K., Janardhan, P., Chakrabarty, D., Ananthakrishnan, S., Ankur Divekar. Changes in quasi-periodic variations of solar photospheric fields: precursor to the deep solar minimum in cycle 23? Sol. Phys., http://dx.doi.org/10.1007/s11207-013-0335-3, in press.

Bornmann, P.L., 1990. Limits to derived flare properties using estimates for the background fluxes: examples from GOES. Astrophys. J. 356, 733–742.
Broomhall, A.-M., Chaplin, W.J., Elsworth, Y., Fletcher, S.T., New, R., 2009. Is the current lack of solar activity only skin deep? Astrophys. J. 700, L162–L165.
Chakrabarty, D., Sekar, R., Narayanan, R., Devasia, C.V., Pathan, B.M., 2005. Evidence for the interplanetary electric field effect on the OI 630.0 nm airglow over low latitude. J. Geophys. Res. 110, A11301, http://dx.doi.org/10.1029/2005JA011221.
Chakrabarty, D., Sekar, R., Narayanan, R., Patra, A.K., Devasia, C.V., 2006. Effects of interplanetary electric field on the development of an equatorial spread F event. J. Geophys. Res. 111, A12316, http://dx.doi.org/10.1029/2006JA011884.
Chakrabarty, D., Sekar, R., Sastri, J.H., Pathan, B.M., Reeves, G.D., Yumoto, K., Kikuchi, T., 2010. Evidence for OI 630.0 nm dayglow variations over low latitudes during onset of a substorm. J. Geophys. Res. 115, A10316, http://dx.doi.org/10.1029/2010JA015643.
Das, U., Pallamraju, D., Chakrabarti, S., 2010. Effect of an X-Class solar flare on the OI 630 nm dayglow emissions. J. Geophys. Res. 115, A08302, http://dx.doi.org/10.1029/2010JA015370.
Davies, K., 1990. Ionospheric Radio. Peter Peregrinus, London.
Donnelly, R.F., 1976. Empirical models of solar flare X-ray and EUV emission for use in studying their E and F region effect. J. Geophys. Res. 81, 4745–4753, http://dx.doi.org/10.1029/JA081i025p04745.
Horan, D.M., Kreplin, R.W., 1981. Simultaneous measurements of EUV and soft X-ray flare emissions. Sol. Phys. 74, 265–272.
Horan, D.M., Kreplin, R.W., Dere, P., 1983. Direct measurements of the gradual extreme ultraviolet emission from large solar flares. Sol. Phys. 85, 303–312.
Kikuchi, T., Hashimoto, K.K., Kitamura, T.-I., Tachihara, H., Fejer, B., 2003. Equatorial counterelectrojets during substorms. J. Geophys. Res. 108 (A11), 1406, http://dx.doi.org/10.1029/2003JA009915.
Le, H., Liu, L., He, H., Wan, W., 2011. Statistical analysis of solar EUV and X-ray flux enhancement induced by solar flares and its implication to upper atmosphere. J. Geophys. Res. 116, A11301, http://dx.doi.org/10.1029/2011JA016704.
Le, H., Liu, L., Wan, W., 2012. An analysis of thermospheric density response to solar flares during 2001–2006. J. Geophys. Res. 117, A03307, http://dx.doi.org/10.1029/2011JA017214.
Leonovich, L.A., Tashchilin, A.V., Portnyagina, O.Y., 2010. Dependence of the ionospheric response on the solar flare parameters based on the theoretical modeling and GPS data. Geomagn. Aeron. 50, 201–210.
Liu, J.Y., Lin, C.H., Chen, Y.I., Lin, Y.C., Fang, T.W., Chen, C.H., Chen, Y.C., Hwang, J.J., 2006. Solar flare signatures of the ionospheric GPS total electron content. J. Geophys. Res. 111, A05308, http://dx.doi.org/10.1029/ 2005JA011306.
Mahajan, K.K., Lodhi, N.K., Upadhayaya, A.K., 2010. Observations of X-ray and EUV fluxes during X-class solar flares and response of upper ionosphere. J. Geophys. Res. 115, A12330, http://dx.doi.org/10.1029/2010JA015576.
Manju, G., Viswanathan, K.S., 2005. Response of the equatorial electrojet to solar flare related X-ray flux enhancements. Earth Planets Space 57, 231–242.
Mendillo, M., Klobuchar, J.A., Fritz, R.B., da Rosa, A.V., Kersley, L., Yeh, K.C., Flaherty, B.J., Rangaswamy, S., Schmid, P.E., Evans, J.V., Schödel, J.P., Matsoukas, D.A., Koster, J.R., Webster, A.R., Chin, P., 1974. Behavior of the ionospheric F region during the greatest solar flare of August 7, 1972. J. Geophys. Res. 7, 665–672, http://dx.doi.org/10.1029/JA079i004p00665.
Mitra, A.P., 1974. Ionospheric Effects of Solar Flares. Springer, New York, p. 294.
Nagata, T., 1966. Solar flare effect on the geomagnetic field. J. Geomag. Geoelectr. 18, 197–219.
Nandi Dibyendu, Andrés Muñoz Jaramillo, Petrus C.H. Martens, 2011. The unusual minimum of sunspot cycle 23 caused by meridional plasma flow variations. Nature, 471, 80-82, http://dx.doi.org/10.1038/nature09786.
Ogawa, H.S., McMullin, D.R., Judge, D.L., Korde, R., 1993. Normal incidence spectrophotometer with high-density transmission grating technology and high efficiency silicon photodiodes for absolute solar extreme-ultraviolet irradiance measurements. Opt. Eng. 32, 3121.
Onwumechili, C.A., 1997. The Equatorial Electrojet. Gordon and Breach Science Publishers, Netherlands, pp. 393–395..
Oshio, M., Fukushima, N., Nagata, T., 1967. Solar flare effects on geomagnetic field. Rep. Ionos. Space Res. Jpn. 21, 77–114.
Raja Rao, K.S., Panduranga Rao, M., 1963. On the location of ionospheric current system causing geomagnetic solar flare effects. J. Atmos. Sci. 20, 498–501.
Rastogi, R.G., Patil, A., 1986. Complex structure of equatorial electrojet current. Curr. Sci. 55, 433–436.
Rastogi, R.G., Pathan, B.M., Rao, D.R.K., Sastry, T.S., Sastri, J.H., 1999. Solar flare effects on the geomagnetic elements during normal and counter electrojet periods. Earth Planets Space 51, 947–957.
Richmond, A.D., Venkateswaran, S.V., 1971. Geomagnetic crochets and associated ionospheric current systems. Radio Sci. 6, 139–164.
Rishbeth, H., Garriot, O.K., 1969. Introduction to Ionospheric Physics. Academic Press.
Ryan, D.F., Milligan, R.O., Gallagher, P.T., Dennis, B.R., Tolbert, A.K., Schwartz, R.A., Young, C.A., 2012. The thermal properties of solar flares over three solar cycles using GOES X-ray observations. Astrophys. J. (Suppl. Ser.) 202, 11 (15 pp.).
Saint-Hilaire, P., Benz, A.O., 2005. Thermal and non-thermal energies of solar flares. Astron. Astrophys. 435, 743–752.
Sastri, J.H., 2002. Penetration electric fields at the nightside dip equator associated with the main impulse of the storm sudden commencement of 8 July 1991. J. Geophys. Res. 107, 1448, http://dx.doi.org/10.1029/2002JA009453.
Scherliess, L., Fejer, B.G., 1999. Radar and satellite global equatorial F region vertical drift model. J. Geophys. Res. 104, 6829–6842.
Simi, K.G., Thampi, S.V., Chakrabarty, D., Pathan, B.M., Prabhakaran Nayar, S.R., Kumar Pant, T., 2012. Extreme changes in the equatorial electrojet under the influence of interplanetary electric field and the associated modification in the low-latitude F region plasma distribution. J. Geophys. Res. 117, A03331, http://dx.doi.org/10.1029/2011JA017328.
Solomon, S.C., 2006. Numerical models of the E-region ionosphere. Adv. Space Res. 37, 1031–1037.
Sutton, E.K., Forbes, J.M., Nerem, R.S., Woods, T.N., 2006. Neutral density response to the solar flares of October and November, 2003. Geophys. Res. Lett. 33, L22101, http://dx.doi.org/10.1029/2006GL027737.
Thome, G.D., Wagner, L.S., 1971. Electron density enhancements in the E- and F-regions of the ionosphere during solar flares. J. Geophys. Res. 76, 6883–6895, http://dx.doi.org/10.1029/JA076i028p06883.
Tsurutani, B.T., Judge, D.L., Guarnieri, F.L., Gangopadhyay, P., Jones, A.R., Nuttall, J., Zambon, G.A., Didkovsky, L., Mannucci, A.J., Iijima, B., Meier, R.R., Immel, T.J., Woods, T.N., Prasad, S., Floyd, L., Huba, J., Solomon, S.C., Straus, P., Viereck, R., 2005. The October 28, 2003 extreme EUV solar flare and resultant extreme ionospheric effects: comparison to other Halloween events and the Bastille Day event. Geophys. Res. Lett. 32, L03S09, http://dx.doi.org/10.1029/2004GL021475.
Zhang, D.H., Mo, X.H., Cai, L., Zhang, W., Feng, M., Hao, Y.Q., Xiao, Z., 2011. Impact factor for the ionospheric total electron content response to solar flare irradiation. J. Geophys. Res. 116, A04311, http://dx.doi.org/10.1029/2010JA016089.